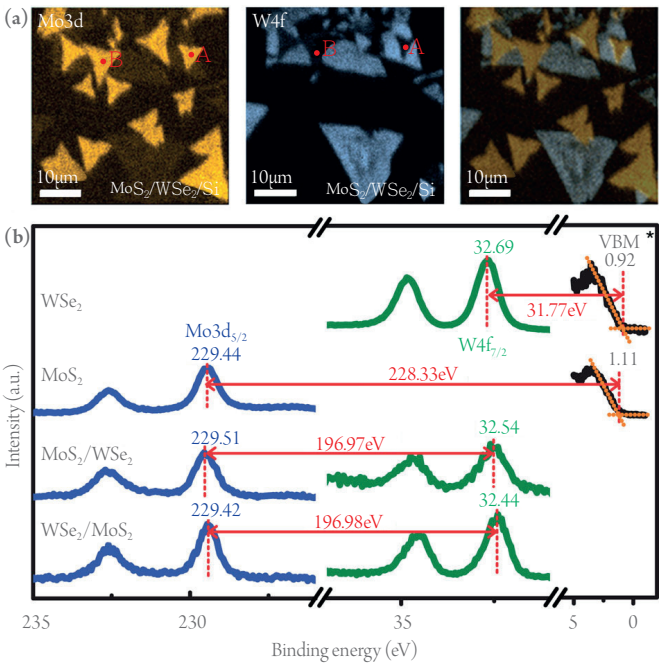

Fig. 3: SPEM measurements on stacked MoS_2/WSe_2 and WSe_2/MoS_2 heterostructures. (a) Mo3d and W4f mappings for the same physical area. The right figure is an overlapped mapping that allows the identification of MoS_2/WSe_2 stacked areas. Points A and B indicate a typical stacking area in which XPS are recorded. (b) Spectra of selected isolated WSe_2 and MoS_2 flakes, stacked MoS_2/WSe_2 and WSe_2/MoS_2 heterostructures. [Reproduced from Ref. 4]

they become direct band-gap semiconductors, which means that their heterojunctions (HJ) are ideal platforms for atomic layer optoelectronic applications. Since HJ band offset is the key parameter for the design of HJ-based electronic or photonic devices, an accurate determination of this parameter is critically important.

To understand the band alignment of TMD, Chih-Kang Shih (University of Texas at Austin, USA) Lain-Jong Li (Academia Sinica/King Abdullah University of Science and Technology, Saudi Arabia) and their co-workers, employed a scanning photoelectron microscopy (SPEM) located at **BL09A1**, to study the band alignment of single layer MoS_2/WSe_2 heterostructure.[4]

Using micro-focused soft X-rays delivered from SPEM (Fig. 3), in conjunction with scanning tunnelling spectroscopy, Shih amd his collaborators determined the band alignment in TMD heterostructures. A type-II alignment in WSe_2/MoS_2 with a valence band offset 0.83 ± 0.07 eV and a conduction band offset 0.76 ± 0.12 eV was determined. The team discovered further that the TMD and its supporting graphite form also a semiconductor/semimetal heterostructure such that a transitivity holds for heterostructures formed between TMD and TMD/graphite.

All works describe above were aimed to elucidate the fundamental physical or chemical properties of vdW materials. Although we are still far from playing with vdW materials as LEGO, all this accumulated knowledge definitely bring us closer to this ultimate goal! (Reported by Chia-Hao Chen)

This report features the works of Ming-Hui Chiu, Chih-Kang Shih, Lain-Jong Li and their co-workers published in Nat. Commun. ***6****, 7666 (2015); of Cheng-Maw Cheng, Ku-Ding Tsuei, Barbaros Özyilmaz and their co-workers published in Sci. Rep.* ***5****, 10025 (2015); and of Chi-Yuan Lin, Shih-Sen Chien and their co-workers published in J. Phys. Chem. C* ***119****, 12910 (2015).*

References

1. A. K. Geim and I. V. Grigorieva, Nature **499**, 419 (2013).
2. C.-Y. Lin, C.-E. Cheng, S. Wang, H. W. Shiu, L. Y. Chang, C.-H. Chen, T.-W. Lin, C.-S. Chang, and F. S.-S. Chien, J. Phys. Chem. C **119**, 12910 (2015).
3. C.-M. Cheng, L. F. Xie, A. Pachoud, H. O. Moser, W. Chen, A. T. S. Wee, A. H. Castro Neto, K.-D. Tsuei, and B. Özyilmaz, Sci. Rep. **5**, 10025 (2015).
4. M.-H. Chiu, C. Zhang, H.-W. Shiu, C.-P. Chuu, C.-H. Chen, C.-Y. S. Chang, C.-H. Chen, M.-Y. Chou, C.-K. Shih, and L.-J. Li, Nat. Commun. **6**, 7666 (2015).

How the Structure of Metallic or Bimetallic Nanocatalysts Affects the Reactivity of a Direct Methanol Fuel Cell

Green chemical energy is a promising source of energy in the pursuit of a natural environment free of pollution. By adopting the decomposition or oxidation of methanol on metallic nanocatalysts supported on oxides in electrochemical cells, the direct methanol fuel cell (DMFC) offers an efficient conversion to electricity and an abundant source of hydrogen, but the structure of a metallic or hetero-metallic nanocatalyst is found to play an important role in the electrochemical reactions in the design of a highly efficient cell or to improve the performance of DMFC operations. In 2015, scientists attempted to bridge the material gap between single metallic or core-shell nanocrystals (NC) and real catalysts by characterizing catalytic processes on supported metal or core-shell nanoclusters. A research team of Meng-Fan Luo (National Central University) investigated the dependence on cluster size of supported rhodium (Rh) nanocatalysts in the decomposition of methanol. As Rh has been widely used and can be alloyed with primary platinum (Pt) catalysts in a DMFC, an investigation of the reaction mechanism and the cluster size in this model system might shed light on the design of a highly efficient catalytic system. From the hetero-structural point of view, another team of Tsan-Yao Chen (National Tsing Hua University) reported the effect of the bimetallic core-shell structure on electrochemical oxidation of MeOH in a full-stack module of a DMFC. Both reports illustrate the importance of catalytic structures on the efficiency of the methanol reaction in a DMFC cell.

From their investiagation,[1-4] the former team demonstrated the decomposition of methanol and methanol-d_4 on Rh clusters supported on an ordered thin film of $Al_2O_3/NiAl(100)$ under UHV conditions with various surface techniques and calculations with density-functional theory. To investigate the correlation between structures of the Rh nanocatalyst and the methanol decomposition, the team performed advanced research in applying X-ray photoemission spectroscopy (PES) at **BL09A2**. In their work, the oxide-supported Rh nanocatalysts were carefully controlled *in situ* to imitate the conditions prepared in the NCU laboratory. To avoid contamination from the reactive gases in air, the research team performed PES measurements *in situ* immediately after the preparation of samples.

As Fig. 1(a) shows, the C 1s PES spectra display the temperature dependence of the decomposition of

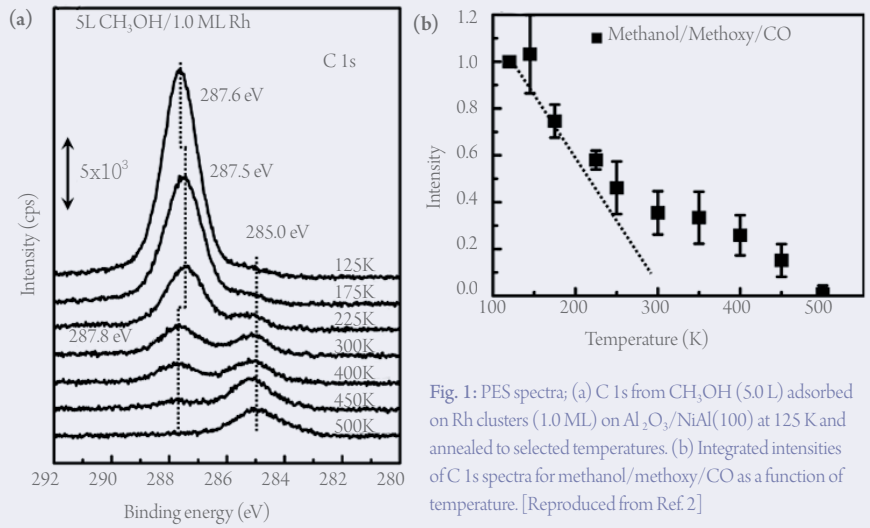

Fig. 1: PES spectra; (a) C 1s from CH_3OH (5.0 L) adsorbed on Rh clusters (1.0 ML) on Al_2O_3/NiAl(100) at 125 K and annealed to selected temperatures. (b) Integrated intensities of C 1s spectra for methanol/methoxy/CO as a function of temperature. [Reproduced from Ref. 2]

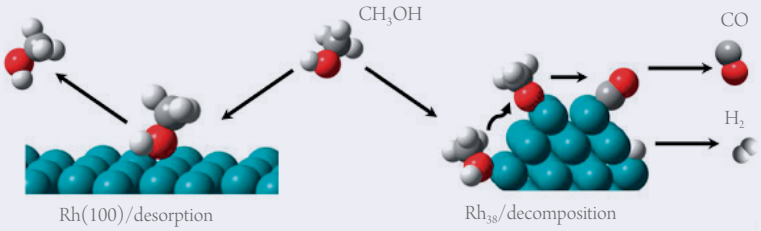

Fig. 2: Formation of CO and hydrogen with optimized structures of CH_3OH and its decomposition fragments on Rh(100) and Rh_{38}. [Reproduced from Ref. 2]

methanol (5.0 L) adsorbed on Rh clusters/Al_2O_3/NiAl(100) (1.0 ML). The PES C 1s spectra provide information about the species methanol/methoxy/CO on the Rh surface at the selected annealing temperature. According to the C 1s signals, the formation of CO vanished about 500 K through dissociation and desorption. A plot of the variation of C 1s integrated intensities as a function of temperature provided an estimate of the probability of dehydrogenation of methanol on the Rh clusters. Figure 1(b) shows two declining lines in the plot. The former indicates the desorption of methanol and the latter primarily the desorption and dissociation of CO. The PES results combined with other experimental and computational results indicate that the methanol on the Rh clusters decomposed via dehydrogenation to CO, which was significantly activated above 200 K, regardless of the cluster size. In contrast, the production of CO and hydrogen (deuterium) per Rh surface site varied notably with the cluster size. As a result, methanol on Rh clusters decomposed through only one channel—dehydrogenation to CO. The schematic diagrams in the Fig. 2 illustrate the results from the DFT calculations. With decreasing cluster size, the activation energy for the scission of the O-H bond in the initial dehydrogenation became smaller than the activation energy for the competing desorption. Therefore, adsorbed methanol on Rh single crystals and large clusters prefers to desorb, whereas that on small clusters to undergo dehydrogenation. The mechanism resembles that on Rh single crystals, but differs from that on supported Pt and Pd nanoclusters, for which scission of the C-O bond serves as an alternative channel.

The structural stability of the nanocatalyst is also critical to affect the performance of the electrochemical reaction in a DMFC. Among the nanocatalysts, the core–shell structure of NC displays the most structural stabilization from the nanometer to the atomic scale. The research team of Tsan-Yao Chen studied various structural configurations of alloyed RuPt and core–shell NC (Ru_{Core}–Pt_{Shell} NC, denoted as Pt_S/Ru_C) for the electrochemical oxidation of MeOH in a full-stack module of a DMFC. To unravel the influence of the core-shell structure on the reactivity of DMFC, the physical structures of the NC were characterized with X-ray absorption spectroscopy at **BL07A1**, **BL17C1**, and **SP12B1**. As Figs. 3(a) and 3(b) show, the X-ray-absorption near-edge structure (XANES) spectra of PtS/RuC NC elucidate the changes of the chemical states and the atomic ordering of Pt and Ru atoms on NC after electrochemical reactions. Figure 3(a) indicates the formation of an ultra-thin Pt oxide on the outermost layer of freshly prepared NC. Compared to alloyed RuPt NC, substantially decreased H_{A^*} and increased H_{B^*} illustrate the reduction of Pt oxides in the redox reaction in MOR and DMFC work cycles. The Ru K-edge XANES spectrum in Fig. 3(b) indicates that the RuO_2 core was shielded by the Pt shell capsule without exposure to the chemisorption of protons. The chemical state and structural evolution were confirmed with Fourier-transformed radial-structure functions for the samples at the Pt L3 and Ru K-edges in Figs. 3(c) and 3(d), respectively. The absence of Pt–O and Pt–Pt_{ox} signals indicates the reduction of Pt oxide. This conformational confinement of Pt_S/Ru_C core–shell NC enhanced the charge donation from the shell Pt to the core Ru, and thus improved the CO tolerance factor to the module durability of the DMFC.

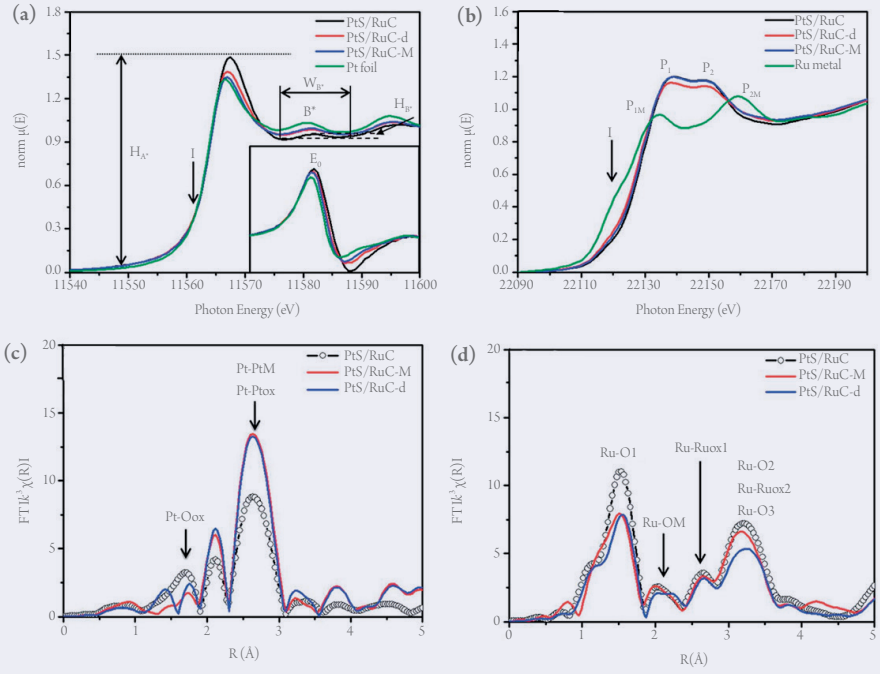

Fig. 3: XANES spectra for NC with and without conducting MOR and DMFC work cycles for Pt_S/Ru_C NC at (a) Pt L3-edge and (b) Ru K-edge. (c) Fourier-transformed radial-structure functions for NC at the Pt L3-edge and (d) Ru K-edge. [Reproduced from Ref. 4]

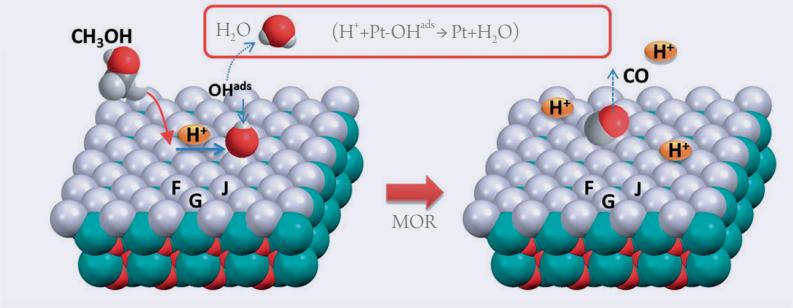

Fig. 4: Bimetallic models of Pt_S/Ru_C NC: Pt on RuO_2 (001) "4×4 RuO_2+ 32 Pt". [Reproduced from Ref. 4]

Figure 4 shows the configuration of Pt_S/Ru_C NC to illustrate the effect of the geometric confinement on the local restructuring in the surface of the core-shell NC during MOR. Chemisorption of CH_3OH on top of the Pt atoms (Pt–CH_3O-H_{ads}) and subsequent decomposition of H^+ from Pt–CH_3OH_{ads} in the core-shell structure proceeds with a small activation energy. The residual CO molecule adhered at both the bridge of the Pt_F–Pt_G sites and the hollow sites after decomposition of H^+ from Pt–CH_3OH_{ads} in the core-shell that elongates the bond between the CO molecule and the sorption sites. This bond weakening leads to substantial dissolution followed by a regrowth of hydrophilic components under mild redox conditions. This geometrical confinement can serve as a highly ordered Pt capsule to protect the core from the redox environment, thus improving the enduring stability of the NC.

These two works not only renew our knowledge about the structural effects of nanocatalysts, apart from the well investigated phenomena of reactivity and durability, but also indicate a new direction to control metallic structure or the core-shell heterostructure, which is the key to achieve a great DMFC fuel cell. (Reported by Yao-Jane Hsu)

This report features the works of Meng-Fan Luo and his co-workers published in ACS Catalysis ***5****, 4726 (2015) and of Tsan-Yao Chen and his co-workers published in J. Mater. Chem. A* ***3****, 1518 (2015).*

References

1. M.-F. Luo, H.-W. Shiu, M.-H. Tien, S. D. Sartale, C. I. Chiang, Y. C. Lin, and Y. J. Hsu, Surf. Sci. **602**, 241 (2008).
2. J. Zhou and D. R. Mullins, J. Phys. Chem. B **110**, 15994 (2006).
3. T.-C. Hung, T.-W. Liao, Z.-H. Liao, P.-W. Hsu, P.-Y. Cai, H. Lee, Y.-L. Lai, Y.-J. Hsu, H.-Y. Chen, J.-H. Wang, and M.-F. Luo, ACS Catal. **5**, 4276 (2015).
4. J.-J. Wang, Y.-T. Liu, I.-L. Chen, Y.-W. Yang, T.-K. Yeh, C.-H. Lee, C.-C. Hu, T.-C. Wen, T.-Y. Chen, and T.-L. Lin, J. Phys. Chem. C **118**, 2253 (2014).
5. T.-Y. Chen, G.-W. Lee, Y.-T. Liu, Y.-F. Liao, C.-C. Huang, D.-S. Lin, and T.-L. Lin, J. Mater. Chem. A **3**, 1518 (2015).

Magnetic Mesocrystals of New Types

Mesocrystals, materials in a new class with nanocrystal superstructures exhibiting directional or translational symmetry, have captured significant attention in the past decade due to their potential for applications of catalytic, electronic, optical, drug-delivery and reaction-precursor applications. Because of their structural nature, the mesocrystals can possess unique properties and functionalities that are distinct from bulk or nano functional materials. Considerable efforts have been made to develop mechanisms of synthesis and to acquire new members of the mesocrystal family, such as oxide, metal and organics, as well as to tailor their various functionalities. In 2015, a research team of Ying-Hao Chu (National Chiao Tung University) demonstrated magnetic mesocrystals of several new types consisting of self-assembled core-shell nanocrystals or nanocrystals embedded in a matrix material via epitaxial growth. The epitaxy enables the alignment of orientations among nanocrystals, forming building blocks of a mesocrystal to enlarge the playground of mesocrystals. According to their recent reports, this team demonstrated a growth method to synthesize self-organized two-dimensional mesocrystals composed of highly oriented magnetic nanocrystals with assistance of shell materials or various matrices. The properties of the mesocrystals were modulated on either varying the core-shell structure or altering the surrounding matrix. To uncover the intriguing functionalities of these mesocrystals, X-ray absorption spectroscopy (XAS) and X-ray magnetic circular dichroism (XMCD) at **BL11A1** were employed to understand the coupling mechanisms between core and shell materials or nanocrystal and matrix, which provide critical insight to tailor the physical properties of mesocrystals.

Considerable efforts have been made to develop mechanisms of synthesis and to acquire new members of the mesocrystal family as well as to tailor their tantalizing functionalities. The challenge to grow core-shell oxide nanocrystals as building blocks for mesocrystals remains in the formation of discrete nanocrystals epitaxially on substrates. In Ref. 1, they employed cobalt oxide (CoO)-cobalt ferrite ($Co_xFe_{3-x}O_4$, CFO) as a model system of self-assembled core-shell building blocks for mesocrystals. CoO is an antiferromagnetic (AFM) material; it can modify the magnetic anisotropy of ferrimagnetic CFO via interfacial exchange coupling. They used $BiCoO_3$/$BiFeO_3$ targets to generate CoO/Fe_3O_4 and Bi_2O_3 species with pulsed-laser deposition (PLD). Fe_3O_4 would notably react further with CoO to form the CFO during the deposition. The greater interfacial energy of Fe_3O_4-STO interfaces plays an essential role to drive Fe_3O_4 to diffuse toward CoO cores with the aid of melted Bi_2O_3. After the deposition, the growth chamber was again evacuated to remove Bi_2O_3, and core-shell mesocrystals were formed. The orientation control of core-shell building blocks can be achieved also with varied morphology and properties of mesocrystals. The magnetic anisotropy strongly reflects the advantages of the orientation control in mesocrystal systems. In addition, the interface of the core-shell mesocrystal can be designed on varying the ratio of core to shell because the exchange coupling at the CFO-CoO interface can modify the magnetic anisotropy of the building blocks and thus the entire mesocrystal. Furthermore, the sequence of core-shell is another parameter to be controlled to tailor the properties of core-shell mesocrystals; CFO(core)-CoO(shell) *inverse* mesocrystals can be fabricated simply on exchanging the deposition sequence of $BiCoO_3$ and $BiFeO_3$.

In this work, as the crystal structures of CoO and CFO are similar, inter-diffusion is expected, which hinders the basic understanding of the mesocrystal system. To provide further information, XAS-XMCD was employed. To determine the value of x in $Co_xFe_{3-x}O_4$ phases, XMCD was applied to determine the valence and magnetic moment of Fe and Co. A magnetic field ± 1 T was applied along the out-of-plane direction of samples and the Poynting vector of X-rays was 30° off the out-of-plane axis. Figures 1(a) and 1(b) show the XMCD results of the CoO and Fe_3O_4 core-